

Full length article

# Sputter-cleaning modified interfacial energetic and molecular structure of DNTT thin film on ITO substrate

Souvik Jana, Subhankar Mandal, Saugata Roy, Md Saifuddin, Satyajit Hazra \*

Saha Institute of Nuclear Physics, A CI of Homi Bhabha National Institute, 1/AF Bidhannagar, Kolkata 700064, India

## ARTICLE INFO

## Keywords:

Organic semiconductor  
 Interfacial energetics  
 Molecular structures  
 Energy level alignment  
 Hole injection barrier  
 Film-growth mode

## ABSTRACT

The effect of natural electrode contamination on interfacial energetic, structure and morphology of  $\pi$ -conjugated organic molecular layers were studied by depositing dinaphthothienothiophene (DNTT) thin films of varying thickness on indium-tin-oxide (ITO) substrates and by using photoelectron spectroscopy, atomic force microscopy and X-ray reflectivity techniques. The DNTT thin film on unclean-ITO surface shows a smaller threshold ionization potential (by  $\sim 0.4$  eV) compared to the film on clean-ITO one. A molecule–substrate interaction, present in the DNTT/clean-ITO system, gives rise to an interfacial dipole and charge transfer, presumably through flat-lying seed-layer at the interface. On further deposition, the interfacial coverage increases, while the molecules on top of the seed-layer take different orientation (mostly edge-on) to form highly-dewetted fibrous-islands of very high-thickness but very low-coverage. Overall, the growth of DNTT film on clean-ITO surface is layer-plus-island-like or Stranski–Krastanov-type. On the other hand, the contamination layer at the DNTT/unclean-ITO interface is found to act as a spacer layer, which reduces the intimate molecule–substrate interaction and also the roughness to give rise an edge-on ordered island-like or Volmer–Weber-type film-growth with reduced hole injection barrier (by  $\sim 0.2$  eV) and better (almost double) film-coverage to make it a more efficient hole injector compared to the clean interface one.

## 1. Introduction

Continuous development and improvement of organic semiconductor (OSC) based devices [1], such as organic photovoltaics (OPV) [2,3], organic light-emitting diodes [4–6], and organic thin film transistors (OTFT) [7–10], in last few years, have intensified the need to understand the metal electrode–organic interfaces as the performances of such devices strongly depend on the efficiency of charge injection from an electrode into the active OSC material [11]. In OSC-based devices, where transparent electrode is essential, indium tin oxide (ITO) is the natural choice [12–15], as it shows very high electrical conductivity (similar to metal) and optical transparency ( $> 80\%$  in the visible region) [16]. Several studies have been carried out on the interface between ITO and different OSCs to get control over the energy level alignment (ELA) at the interface [13–15]. However, the role of the natural surface contamination, which can take place due to the exposure of organic thin films or the patterned electrode surfaces into the ambient or poor vacuum conditions prior to the device fabrication [17,18], on the ELA at OSC/ITO interface has not been studied so far. A contamination layer, consisting of  $N_2$ ,  $O_2$ ,  $H_2O$ , and hydrocarbons, generally formed on the electrode surface under such exposer, which can not only tune the ELA at OSC/electrode interface

but also the conformation and orientation of the molecule and the top surface morphology of the thin film [17–21]. Hence it is important to study the differences in the OSC/ITO interface energetics made by this unavoidable environmental contamination.

Dinaphthothienothiophene (DNTT), on the other hand, has recently emerged as a very promising material for potential application in OSC-based device due to its good air and thermal stability [8,22] and very high hole mobilities ( $\sim 3.1$   $\text{cm}^2 \text{V}^{-1} \text{s}^{-1}$  for thin film-based OTFT and  $\sim 8.3$   $\text{cm}^2 \text{V}^{-1} \text{s}^{-1}$  for single crystal-based OTFT) [23,24]. Such DNTT molecule is a highly  $\pi$ -extended heteroarene, which consists of six fused aromatic rings and two sulfur atoms located at the central heteroaromatic rings [25,26] (as shown schematically in Fig. S1 of the Supporting Information). Single crystal of DNTT is known to form through a packing of molecules in herringbone fashion [27,28], which plays an important role in its charge transport properties. Strong intermolecular interaction and overlapping of its frontier molecular orbital were also found in this molecule which makes it more promising for its use as an active material in the high-performance OTFT and also in OPV [26,29,30]. Apart from this intermolecular interaction; the molecule–electrode interaction also plays important role in deciding the molecular orientation, molecular conformation, and coverage of

\* Corresponding author.

E-mail address: [satyajit.hazra@saha.ac.in](mailto:satyajit.hazra@saha.ac.in) (S. Hazra).

such molecules near the film–substrate interface, which then controls the ELA at the interface and its device performances [30–33]. The molecule–electrode interaction again largely depends on the cleanliness of the electrode surface. So, understanding the effect of the electrode contamination on the ELA at the interface and the morphology of the film, especially at the interface, is crucial for efficient charge injection and extraction from the electrode. Unfortunately, not much work have been carried out to understand the effect of electrode contamination, especially transparent electrode contamination, on the ELA and interfacial morphology of DNTT thin film.

Here, this issue has been addressed by studying the electronic structures of DNTT thin film of varying thickness (from sub-monolayer to multilayer) on unclean and clean ITO substrates using in situ ultraviolet and X-ray photoelectron spectroscopic (UPS and XPS) techniques and subsequently studying the surface morphology of few selected films using atomic force microscopic (AFM) technique. Indeed, the present study shows a noticeable effect of environmental contamination on the electronic structure and morphology of DNTT thin film on ITO. In fact, the adventitious contamination layer present on the ITO surface was found to act as a spacer layer between the ITO surface and DNTT molecular layer, which changes the intimate molecule–electrode interaction to affect the interfacial dipole formation mechanism as well as the ELA and the morphology. The unclean ITO surface, having lower work function, shows closer highest occupied molecular orbital (HOMO) level w.r.t. the Fermi level, lower threshold ionization potential ( $IP_{th}$ ) and better coverage of the DNTT film compared to those on the clean ITO surface. The possible reasons of such result and its implications on the device performances are discussed.

## 2. Experimental details

The electronic structures of the DNTT/ITO interfaces, with or without environmental contamination layer, were characterized systematically by using photoelectron spectroscopic techniques inside an ultra-high vacuum (UHV) chamber (Omicron Nanotechnology, of base pressure  $\sim 1.5 \times 10^{-9}$  mbar). The UHV chamber was equipped with an EA125 hemispherical energy analyzer and two monochromatic photon sources [34]. A He gas discharge lamp having photon energy,  $E_0 = 21.2$  eV (He I) was used as a UV light source to get the UPS spectra, where the spectrometer energy resolution was  $\sim 0.1$  eV. A sample bias of  $-8.0$  V was applied during UPS measurements to determine the higher binding energy cut-off (HBEC). A monochromatic Al  $K\alpha$  (of  $E_0 = 1486.6$  eV) was used as X-ray source for XPS measurements, where the corresponding spectrometer resolution was  $\sim 0.8$  eV. All the UPS and XPS spectra were collected keeping the sample at room temperature.

ITO-coated glass substrates (from Sigma-Aldrich, having a sheet resistance of  $\sim 10 \Omega \text{ cm}^{-2}$ ) were used for this experiment. Two sets of substrates (each of size about  $10 \times 10 \text{ mm}^2$ ) were sonicated first in acetone and then in ethanol to remove the organic contaminants and finally dried with a flow of dry nitrogen before inserting them into the UHV chamber. One set substrates was further treated with  $\text{Ar}^+$  ion sputtering until a clean surface of ITO was obtained. The cleanliness of the ITO substrate was monitored through XPS spectra (and confirmed from the absence of the C 1s core level peak in the spectrum as shown Fig. S2 of the Supporting Information). This sputter-clean substrates were designated as “clean-ITO”, while the only organic clean substrates were designated as “unclean-ITO”. These substrates were then placed inside a high-vacuum deposition chamber (of base pressure  $\sim 2.0 \times 10^{-8}$  mbar) that is attached with the UHV characterization chamber. Thin films of different cumulative nominal thicknesses ( $D_{CN} = 3, 6, 9, 16, \text{ and } 32 \text{ \AA}$ ) were deposited in steps on both types of substrates by thermal evaporation technique using Knudsen effusion cell containing DNTT (of purity  $\approx 99\%$  from Sigma-Aldrich) in a quartz crucible. Thin films of a nominal thickness,  $D_N = 10 \text{ nm}$ , were also deposited on both types of substrates. A pre-calibrated quartz crystal microbalance was used to monitor the nominal thickness. The deposition was carried out

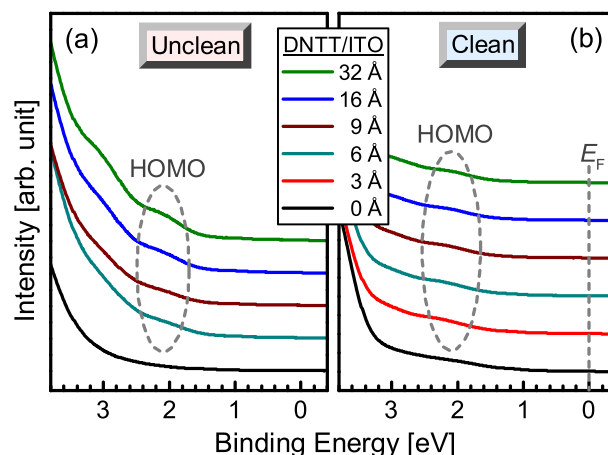


Fig. 1. HOMO region of the UPS spectra for the DNTT thin films of different thickness ( $D_{CN}$ ) on (a) unclean and (b) clean-ITO substrates. HOMO level corresponding to the DNTT film is indicated.

at a fixed evaporation rate ( $\sim 1 \text{ \AA min}^{-1}$ ) keeping the substrates at room temperature. Thin films of different  $D_{CN}$ -values were characterized by in-situ XPS and UPS techniques after each steps of deposition. Sn  $3d_{5/2}$  level (binding energy of 486.5 eV) [35] was chosen as the reference level for the fine calibration of other core levels. For a detailed analysis of the XPS spectra, CASAXPS software was used and the UPS spectra were analyzed using the OriginPro software. The XPS background correction was done using the Shirley method and all the XPS core-level spectra were fitted with a Gaussian–Lorentzian product function.

Surface morphologies of DNTT thin films (of  $D_{CN} = 32 \text{ \AA}$ ) on unclean and clean-ITO substrates were mapped using an atomic force microscope (Nano-observer, CSI) [34,36,37]. AFM images were collected in tapping mode using Au-coated Si tip (radius of curvature  $\sim 10 \text{ nm}$  and resonance frequency  $\sim 60 \text{ kHz}$ ). The images were taken in several regions of the film with different scan areas to check the homogeneity of the surface morphology of the samples. The AFM images were processed and analyzed by WSXM software [38].

X-ray reflectivity measurements of DNTT thin films (of  $D_N = 10 \text{ nm}$ ) on unclean and clean-ITO substrates were performed using a X-ray diffractometer (Smartlab, Rigaku) [39,40], which was equipped with a copper source (sealed tube) followed by a Johansson Ge crystal and a parabolic multilayer mirror to obtain an intense parallel beam of Cu  $K_{\alpha 1}$  radiation (wavelength 1.5406  $\text{ \AA}$ ). The scattered beam was detected using a point (NaI scintillation) detector. Data were taken in the specular condition; that is, the incident angle ( $\theta$ ) is equal to the reflected angle ( $\theta$ ), and both are in the scattering plane.

## 3. Results and discussion

### 3.1. Electronic structure

The effect of ITO contamination on the electronic structures of the DNTT thin films, as investigated systematically using UPS and XPS techniques, are presented here.

#### 3.1.1. UPS study

The HOMO region of the UPS spectra for the DNTT thin films of different  $D_{CN}$ -values on unclean and clean-ITO substrates are shown in Fig. 1. The presence of DNTT-related HOMO peak, close to the Fermi level ( $E_F$ ), though weak due to the higher substrate background signals, is evident in Fig. 1. To get a clear view about the HOMO level, the substrate background subtracted and intensity normalized spectra for the DNTT thin films on ITO substrates are shown in Fig. 2. An increase in the HOMO peak intensity with the increase in the film thickness (as

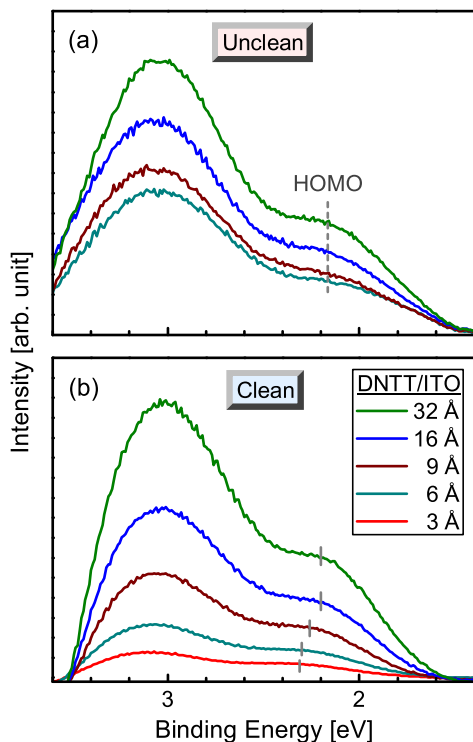


**Fig. 2.** Substrate background-subtracted HOMO region of the UPS spectra for the DNTT thin films of different thickness ( $D_{CN}$ ) on (a) unclean and (b) clean-ITO substrates. HOMO peak positions for the DNTT films are indicated.

expected) is clearly evident for the DNTT films on both the substrates. The HOMO peak position remains unchanged for the films on the unclean-ITO substrate, whereas a shifting tendency towards the lower binding energy is observed for the films on clean-ITO substrate with the increase of film thickness. For the latter, a small shift of around  $-0.1$  eV is evident for the  $32 \text{ \AA}$  film compared to the  $3 \text{ \AA}$  film. The hole injection barrier height ( $\phi_{bh}$ ), defined as the energy difference between the onset of the HOMO level and  $E_F$ , is found higher for the thin film on the clean-ITO substrate ( $\sim 1.7$  eV) compared to that on the unclean one ( $\sim 1.5$  eV), which can be correlated with the different structures of the molecules near the interface arising from different interaction.  $\phi_{bh}$  remains almost unchanged for further deposition on the unclean-ITO substrate but decreases for further deposition on clean-ITO substrate. Around  $0.1$  eV shift, towards lower binding energy, was observed for the  $32 \text{ \AA}$  film compared to the  $3 \text{ \AA}$  film. This change in the  $\phi_{bh}$  value is an indication in the change of the molecular structure along thickness. Essentially the HOMO region results indicate that the structure of the molecules on unclean-ITO substrate remains unchanged with film thickness, while on clean-ITO substrate, the structure near the interface is different from the remaining top part of the film. The structure of the molecules on top part resembles more to the structure of the molecules on the unclean-ITO substrate.

The HBEC region of the UPS spectrum is another important part, which provides information about the vacuum level (VL) or the work function of the surface, following the relation

$$E_{VL} = E_0 - (E_{HBEC} - E_F) \quad (1)$$

where  $E_{VL}$  and  $E_{HBEC}$  represent VL and HBEC, respectively. Such HBEC region of the UPS spectra for the DNTT thin films of different  $D_{CN}$ -values on unclean and clean-ITO substrates are shown in Fig. 3. The spectra of the bare substrates are also included in this figure to show the effect of the cleanliness of the substrate on its surface work function. The work function for the clean-ITO is found around  $4.5$  eV and that of the unclean one is about  $4.1$  eV, which agrees well with reported

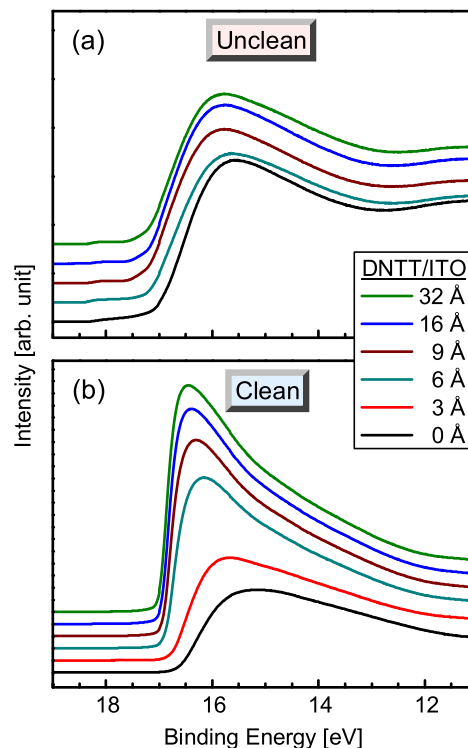


**Fig. 3.** HBEC region of the UPS spectra for the DNTT thin films of different thickness ( $D_{CN}$ ) on (a) unclean and (b) clean-ITO substrates.

values [41]. A noticeable reduction (of about  $0.4$  eV) in the work function or VL is observed for the clean-ITO substrate w.r.t. the unclean one. The reduction of the work function in the unclean one can be explained by the pillow effect or in other words the suppression of the surface component of electron wave function [20]. A change in the VL of about  $-0.2$  eV is observed after deposition of  $3 \text{ \AA}$  thick DNTT film on the clean-ITO substrate, which becomes about  $-0.3$  eV for  $32 \text{ \AA}$  thick film. A very small shift in the VL (around  $-0.1$  eV) is observed for the deposition of  $6 \text{ \AA}$  thick film on unclean-ITO substrate, which becomes around  $-0.2$  eV for  $9 \text{ \AA}$  thick film. No VL shift is observed upon further deposition, which indicates the absence of any band bending in the thickness range ( $9$ – $32 \text{ \AA}$ ). It can be noted that a VL shift (of  $-0.2$  eV) occurs for the  $3 \text{ \AA}$  thick film on clean-ITO substrate and for similar shift on the unclean-ITO substrate,  $9 \text{ \AA}$  thick film is needed.

The major shifting of the VL in the initial step of deposition ( $3 \text{ \AA}$ ) on clean-ITO substrate can be associated with the interface dipoles arising from large molecular coverage. However, the strength of the dipoles at DNTT/ITO interfaces is found considerably smaller than that measured at DNTT/metal interfaces [30,32]. This is quite obvious as the chemical nature of the ITO surface is quite different from that of the metal surface and also the ITO has a very low density of states near the Fermi Level as compared to the metal substrates. There are several mechanisms, such as partial charge transfer, push-back, permanent dipoles or chemical interaction at the interface, etc., which can give rise to the interface dipoles. The presence of push-back effect at the organic semiconductor/ITO interface was observed before [14]. In the present case, interface dipoles at the DNTT/clean-ITO interface are likely to be formed due to the combined effect of partial charge transfer and push-back effect. The effect of charge transfer at the DNTT/clean-ITO interface will be verified in the XPS section. The unclean-ITO surface, on the other hand, was already affected by the push-back effect from the contamination layer, as obvious from the reduction of the work function value, and thus upon DNTT deposition, it shows a relatively smaller shift in the VL compared to that on the clean one. In addition,

the molecular orientation on unclean-ITO surface may be different compared to those on the clean one, which may give rise smaller interfacial coverage and hence smaller shift in the VL.

The threshold ionization potential ( $IP_{th}$ ), obtained from the HOMO and vacuum levels, is found around 6 eV for the 3 Å thick DNNT film on clean-ITO surface, which decreases to 5.8 eV for the 32 Å thick DNNT film. A slightly higher value of  $IP_{th}$  for the DNNT on clean-ITO surface compared to the bulk DNNT on Au surface [42] is possibly related to the different interfacial behavior and molecular orientation and packing. Whereas the  $IP_{th}$  value for the 6 Å thick DNNT film on unclean-ITO surface is found around 5.5 eV, which reduces to 5.4 eV for the 32 Å thick DNNT film, similar to that reported for the bulk DNNT. Here the environmental contamination layer on the unclean-ITO probably acts as a spacer layer to screen the ITO related interfacial behavior, which was otherwise present in the clean-ITO, to have the  $IP_{th}$  value closer to the bulk one.

### 3.1.2. XPS study

To understand the effect of the substrate cleanliness on the interaction between DNNT and ITO substrate, C 1s and S 2p core level spectra collected after each steps of deposition on unclean and clean ITO substrates are presented in Fig. 4 and Fig. 5, respectively. The primary contamination at the unclean-ITO surface are mostly carbon, which came from the ambient exposure of the substrates. Additionally, the presence of a small amount of organic residue (arising from the organic solvent used for primary cleaning) and a small amount of moisture are obvious (from Fig. S3 of the Supporting information). An intense C 1s peak, known as adventitious carbon, is evident on unclean-ITO substrate. This C 1s region of the XPS spectra for the unclean-ITO substrate can be deconvoluted into two main peaks, namely arising from C–C (284.9 eV) and C–O (286 eV), which are generally present on any surface [18,43]. After deposition of DNNT molecules on unclean-ITO surface, a noticeable asymmetry is observed in the C 1s peak. Such asymmetry comes due to the convolution of the DNNT carbons with the adventitious carbons. Accordingly, the C 1s peak was fitted with those two peaks. As expected, the relative intensity of DNNT-related peak increases with the increase of DNNT deposition (see Fig. 4(a)). No shift in the position of the DNNT-related C 1s and S 2p peaks is observed with increasing film-thickness for the films on the unclean-ITO substrate. However, a gradual shift towards the lower binding energy is observed for the films on the clean-ITO substrate. A small shift of around 0.2 eV in the C 1s peak is observed for the 32 Å thick film w.r.t. the 3 Å one. In case of S 2p peak, the shift is around 0.4 eV. This small gradual shift towards lower binding energy with the increasing deposition amount is a signature of a partial charge transfer at the DNNT/clean-ITO interface. The contamination layer at the DNNT/unclean-ITO interface, however, restricts the interaction and hence the charge transfer at this interface. The direction of core level shift with deposition on clean-ITO indicates that the charge transfer takes place from organic molecules to the ITO surface. So, according to the induced density of interface states (IDIS) model, the Fermi level of this ITO surface was initially below the charge neutrality level (CNL) of the organic film [17], as a result the interface vacuum level shifted to the downward direction (as observed in Fig. 3). The decreasing tendency of the FWHM of both (C 1s and S 2p) core level peaks of DNNT with increasing film thickness on the clean-ITO surface also suggests that there is an increase in the crystallinity or ordering of DNNT molecules in each domain with further deposition. In the intensity normalized S 2p core level spectra it is observed that, the peak intensity in the case of DNNT/unclean-ITO system is greater than that of the DNNT/clean-ITO system, which suggests that the film coverage on the unclean surface is higher than that on the clean surface.

### 3.2. Molecular structure

The role of ITO contamination in the molecular structures and morphology of the DNNT thin films, investigated using AFM and XR techniques, are presented here.

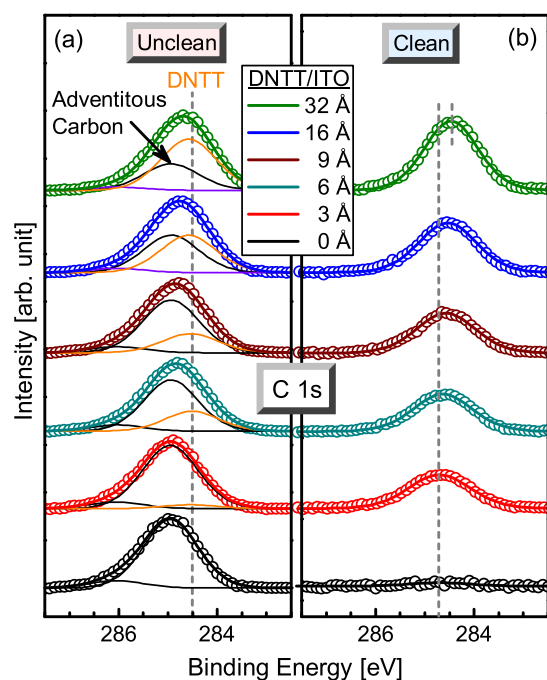


Fig. 4. C 1s core level spectra for the DNNT thin films of different thickness ( $D_{CN}$ ) on (a) unclean and (b) clean-ITO substrates showing the growth of DNNT carbon peak, suppressing the adventitious carbon peak, with film thickness on unclean-ITO substrate and shift of carbon peak position with film thickness on clean ITO substrate.

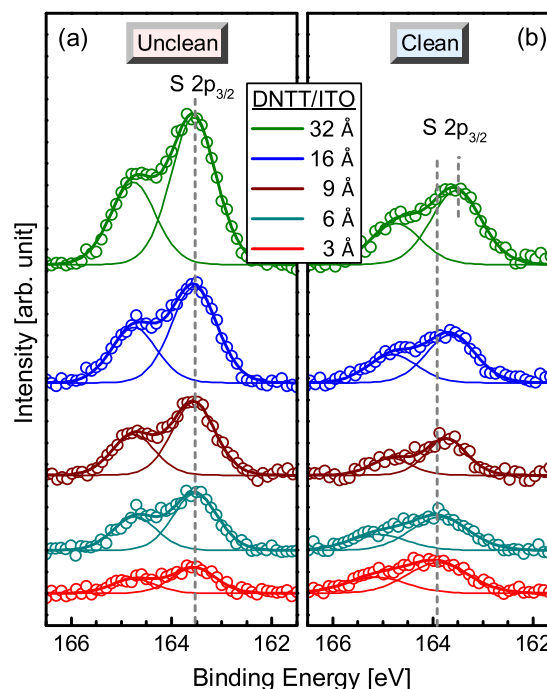


Fig. 5. S 2p core level spectra for the DNNT thin films of different thickness ( $D_{CN}$ ) on (a) unclean and (b) clean-ITO substrates. Peak positions and their shift with film thickness on clean-ITO substrate are indicated.

#### 3.2.1. AFM study

To understand the impact of the cleanliness of ITO surface on the structure and morphology of the DNNT films, AFM images collected for the thick ( $D_{CN} = 32$  Å) DNNT films on clean and unclean ITO substrates are shown in Fig. 6. A fiber-like structure is observed on the clean-ITO surface with very low coverage (around 10%), where

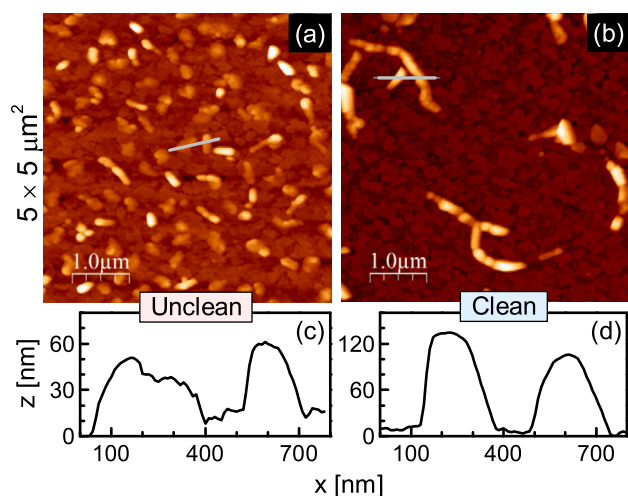


Fig. 6. AFM images (of size  $5 \times 5 \mu\text{m}^2$ ) of relatively thick ( $D_{\text{CN}} = 32 \text{ \AA}$ ) DNTT films on (a) unclean and (b) clean-ITO substrates. (c) and (d) Height variations along the lines drawn through the respectively images.

the average height and width of the fibers are around 115 nm and 275 nm, respectively. A island-like structure is found on the unclean-ITO surface with low coverage (around 20%), where the average height of the island is around 55 nm. The increased coverage of DNTT film on the unclean-ITO surface supports well the XPS and XR results. Such highly dewetted structures (fiber and island) on both the substrates is a signature of island-type growth of DNTT thin films. The highly dewetted DNTT structure observed before on different surface was attributed to the interfacial stress formed between the first layer and the layer on top of it having different molecular orientations [26,30,32]. Similar phenomenon is expected on clean-ITO surface, where the molecules at the first layer may adsorb in flat-like orientation to cover the surface and maximize the interfacial interaction. In the subsequent layers different molecular orientation enhances the strain and reduces the wettability of the film. That is the growth of DNTT on clean-ITO may be more like layer-plus-island type. On the other hand, in case of unclean-ITO, the contamination layer reduces the interfacial interaction between DNTT molecules and the ITO surface, which possibly makes the orientation of the molecules (stand-up) more suitable for bulk-like structure. Such island-like structure of DNTT likely to decrease the interfacial coverage but increase the film coverage, as evident from the topography. The contamination layer also reduces the undulation of the ITO surface that might also have an effect on the betterment of the coverage of the DNTT film.

### 3.2.2. XR study

To get the structural information of the DNTT film along  $z$ -direction and also to understand the effect of the contamination layer on the molecular structure, XR profiles collected for thick ( $D_{\text{N}} = 10 \text{ nm}$ ) DNTT films on unclean and clean-ITO substrates are shown in Fig. 7. A peak near  $2\theta = 5.4^\circ$ , though weak, is observed in the films deposited on both the substrates, which corresponds to the  $d$ -spacing of  $16.3 \text{ \AA}$  similar to the molecular length. This represents (001) Bragg peak, which essentially substantiates the stand-up or edge-on oriented ordering of the molecules as observed before on the ITO surface [44], Si/SiO<sub>2</sub> surface [45] and also on some other surfaces [26,32]. The lower intensity of the Bragg peak on the clean-ITO surface, compared to the unclean one (as evident from Fig. S4 of the Supporting Information), is probably associated with the fact that it has a seed-layer having molecules in other (flat-lying) orientation and/or a lower film-coverage, as observed from the AFM images and also from the HOMO peak intensity.

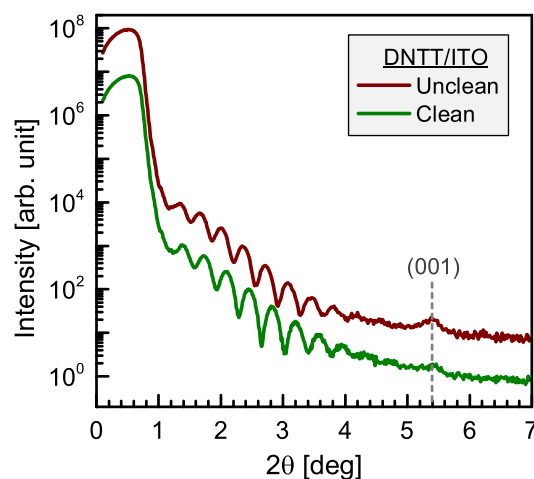


Fig. 7. XR profiles of thick ( $D_{\text{N}} = 10 \text{ nm}$ ) DNTT films on unclean and clean-ITO substrates. Curves are shifted vertically for clarity. The presence of (001) Bragg peak corresponding to the DNTT film is indicated.

## 4. Overall picture and conclusions

The energy-level diagrams of the DNTT thin films of different thickness on unclean and clean-ITO surfaces and the possible configuration, organization and coverage of the DNTT molecules at the interface and above, as modeled using the information obtained from the complementary UPS, XPS, AFM, and XR techniques and some analogy found in the literature, are shown schematically in Fig. 8 to visualize the overall picture.

Formation of interfacial dipoles at the DNTT/clean-ITO interface is obvious (from the shift of VL), which is due to the combined effect of the well known push-back effect arising from the Pauli repulsion of electronic wave-function and a partial charge transfer. The latter is evident from a small shift of the core level (C 1s and S 2p) spectra. Whereas, the formation of weak interface dipoles at the DNTT/unclean-ITO interface (evident from small shift of VL) is related to the push-back effect only as there is no charge transfer at the interface (confirmed from the XPS core level spectra). This is expected as there is a spacer layer, which decouple the electron wave function between ITO surface and DNTT molecules and thus restricts the interaction and the charge transfer.

The interfacial dipoles are very influential for the ELA. A large interfacial dipole generally increases the distance between the Fermi level and the onset of HOMO band, i.e. the  $\phi_{\text{Bh}}$ -value [20]. This is observed in case of DNTT/clean-ITO interface (Fig. 8(b)), where the value of  $\phi_{\text{Bh}}$  is found around 1.7 eV. The weaker interfacial dipole decreases the  $\phi_{\text{Bh}}$ -value, which is ( $\sim 1.5 \text{ eV}$ ) observed for the DNTT/unclean-ITO interface (see Fig. 8(a)). Another important parameter, relevant to the ELA at the interface, is the  $\text{IP}_{\text{th}}$ . This also got affected by the substrate contamination layer. Accordingly, the  $\text{IP}_{\text{th}}$ -value of the unclean-ITO substrate is found less ( $\sim 0.4 \text{ eV}$ ) compared to the clean-ITO one and such difference is almost maintained even after DNTT deposition (see Fig. 8).

It can be noted that depending on the type of the substrate surface, the adsorption geometry of the DNTT molecules at the interface can be very much different. It was observed before that, for a clean and flat Au(111) surface, DNTT molecules at first show a closely-packed (herringbone-like) flat-laying adsorption geometry, where the molecular backbone are oriented almost parallel to the substrate surface. In the subsequent layer, molecules are little tilted as compared to the molecules in the seed-layer to form a possible bulk crystalline structure (12 $\bar{1}$ ) [46]. Whereas on a clean polycrystalline (pc)-Au surface, DNTT molecules at first adsorb in a flat-like face-on orientation following the

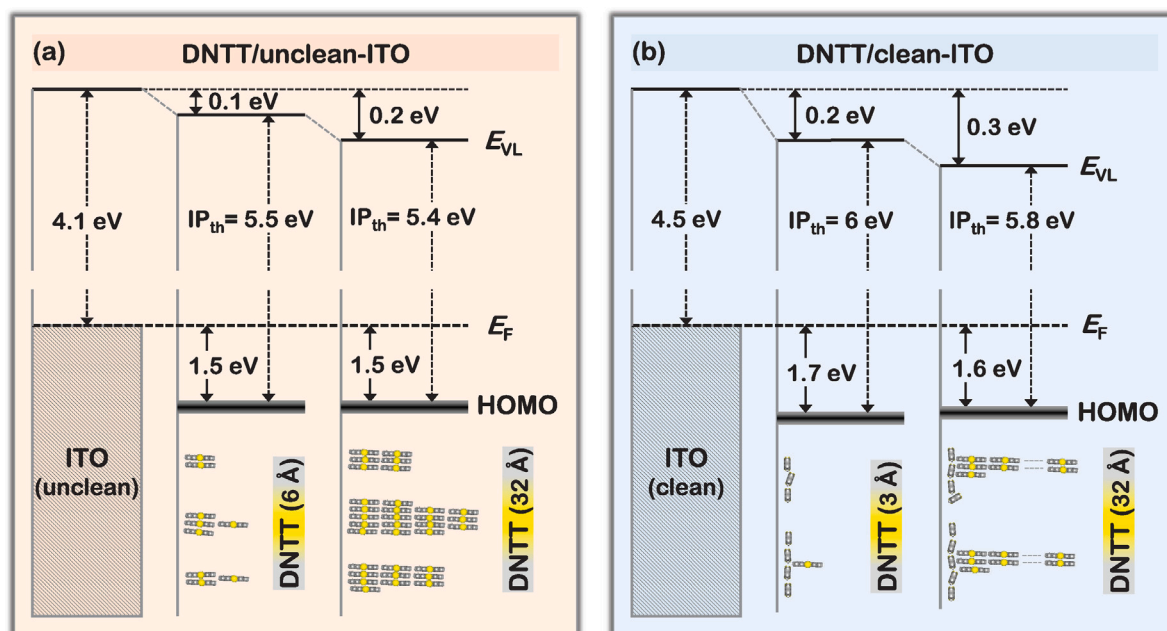


**Fig. 8.** Energy-level diagrams of DNTT thin films of different nominal thicknesses and their possible molecular configuration, organization, and coverage at the interface and above on (a) unclean and (b) clean-ITO substrates, as predicted from UPS, XPS, AFM, and XRD measurements.

surface undulation. In the subsequent deposition, where it is impossible to form bulk crystalline structure with  $(12\bar{1})$  planes because of the undulation of the pc-Au surface, molecules follow up-right orientation to form other preferred bulk crystalline phase with  $(001)$  plane [30,32].

Here also the orientation and the organization of the DNTT molecules on two different ITO surfaces seem to be different. For the nearly monolayer deposition, the molecules on the clean-ITO surface mostly adsorb in flat-like orientation to form a seed-layer similar to that observed on various metallic surfaces [30,32]. This increases the interfacial coverage to have an appreciable change in the VL (around  $-0.2$  eV) and also helps in the charge transfer (as evident from the major change in the VL). On further deposition, the interfacial coverage increases (as evident from the further change in the VL), while the molecules on top of the seed-layer take different orientation (mostly edge-on, as evident from XR data) to form very high-thickness but very low-coverage layer (evident from AFM images) as shown schematically in Fig. 8(b). Overall the growth of DNTT film on clean-ITO surface is layer-plus-island or Stranski–Krastanov (SK) type [47–50]. On the other hand, the molecules on the unclean-ITO surface, without having any interaction and having relatively smaller roughness due to the contaminated spacer layer, seem to adsorb in edge-on orientation (evident from XR data) to follow the bulk-like structure from the beginning. This gives rise to small interfacial coverage at the early stages of deposition (evident from small VL shift), but relatively better film-coverage at the later stages of deposition (evident from AFM images) as shown schematically in Fig. 8(a). Overall the growth of DNTT film on unclean-ITO surface is more like island or Volmer–Weber (VW) type [47–50].

In conclusion, the effect of substrate contamination on the ELA at the DNTT/ITO interface and also on the thin film growth mechanism were studied systematically. The contamination layer on the ITO surface partially suppresses the surface component of electron wave function, which normally tails into the vacuum at the ITO surface, to reduce the work function of the ITO surface, resulting in a less reactive interface. This layer also found to prevent the intimate organic–electrode interaction, which dominates at the clean interface causing a higher hole injection barrier that is a very important parameter in the context of charge transport in the device structure of organic semiconductors. According to the IDIS model, the less intimate contact between organic molecule and electrode substantially reduces

the density of states around CNL of the organic molecules, resulting in a weaker pinning of the Fermi level around CNL and, consequently, the interface energetics is much closer to the vacuum-level alignment (Fig. 8) [17]. In the present case, the contaminated ITO substrate with lower work function gives a weaker interfacial dipoles, resulting in a smaller  $\phi_{\text{BH}}$  as compared to the clean interface and also an  $\text{IP}_{\text{th}}$  which is close to the value of bulk DNTT and comparably lower (around  $0.4$  eV) than the DNTT on clean surface. The crystallinity of the DNTT film is found higher for the unclean surface where the film coverage is better than that on the clean surface. Overall, the electronic structure and thin film structure of DNTT molecules on ITO substrate are found to influence by the interface cleanliness, which are of immense importance for controlling the performances of the organic semiconductor-based devices.

#### CRediT authorship contribution statement

**Souvik Jana:** Data curation, Formal analysis, Investigation, Methodology, Writing – original draft. **Subhankar Mandal:** Data curation, Formal analysis. **Saugata Roy:** Investigation. **Md Saifuddin:** Investigation. **Satyajit Hazra:** Conceptualization, Supervision, Validation, Visualization, Writing – review & editing.

#### Declaration of competing interest

The authors declare that they have no known competing financial interests or personal relationships that could have appeared to influence the work reported in this paper.

#### Data availability

Data will be made available on request.

#### Acknowledgments

The authors thank Mr. G. Sarkar and Dr. Ramkrishna Dev Das for their technical support and Prof. Mrinmay K Mukhopadhyay for providing XR facility. S.M. acknowledges Council of Scientific & Industrial Research (CSIR), India and M.S. acknowledges University Grant Commission (UGC), India for providing research fellowships.

## Appendix A. Supplementary data

Supplementary material related to this article can be found online at <https://doi.org/10.1016/j.apsusc.2024.159368>. Supplementary information, namely structural schematic of a DNNT molecule, XPS survey and core level spectra of ITO substrates, and Bragg peaks of the DNNT films on ITO substrates, associated with this article can be found.

## References

- H. Liu, D. Liu, J. Yang, H. Gao, Y. Wu, Flexible electronics based on organic semiconductors: from patterned assembly to integrated applications, *Small* (2023) 2206938.
- A.W. Hains, Z. Liang, M.A. Woodhouse, B.A. Gregg, Molecular semiconductors in organic photovoltaic cells, *Chem. Rev.* 110 (2010) 6689–6735.
- Y. Cui, H. Yao, L. Hong, T. Zhang, Y. Tang, B. Lin, K. Xian, B. Gao, C. An, P. Bi, W. Ma, J. Hou, Organic photovoltaic cell with 17% efficiency and superior processability, *Natl. Sci. Rev.* 7 (2020) 1239–1246.
- L. Xiao, Z. Chen, B. Qu, J. Luo, S. Kong, Q. Gong, J. Kido, Recent progresses on materials for electrophosphorescent organic light-emitting devices, *Adv. Mater.* 23 (2011) 926–952.
- W. Brütting, J. Frischeisen, T.D. Schmidt, B.J. Scholz, C. Mayr, Device efficiency of organic light-emitting diodes: Progress by improved light outcoupling, *Phys. Stat. Sol. A* 210 (2013) 44–65.
- C.-Y. Chan, M. Tanaka, Y.-T. Lee, Y.-W. Wong, H. Nakanotani, T. Hatakeyama, C. Adachi, Stable pure-blue hyperfluorescence organic light-emitting diodes with high-efficiency and narrow emission, *Nature Photon.* 15 (2021) 203–207.
- O.A. Melville, B.H. Lessard, T.P. Bender, Phthalocyanine-based organic thin-film transistors: a review of recent advances, *ACS Appl. Mater. Interfaces* 7 (2015) 13105–13118.
- Y. Huang, X. Gong, Y. Meng, Z. Wang, X. Chen, J. Li, D. Ji, Z. Wei, L. Li, W. Hu, Effectively modulating thermal activated charge transport in organic semiconductors by precise potential barrier engineering, *Nature Commun.* 12 (2021) 21.
- R.R. Cranston, B. King, C. Dindault, T.M. Grant, N.A. Rice, C. Tonnelé, L. Muccioli, F. Castet, S. Swaraj, B.H. Lessard, Highlighting the processing versatility of a silicon phthalocyanine derivative for organic thin-film transistors, *J. Mater. Chem. C* 10 (2022) 485–495.
- U. Zschieschang, U. Waizmann, J. Weis, J.W. Borchert, H. Klauk, Nanoscale flexible organic thin-film transistors, *Sci. Adv.* 8 (2022) eabm9845.
- A. Kumatani, Y. Li, P. Darmawan, T. Minari, K. Tsukagoshi, On practical charge injection at the metal/organic semiconductor interface, *Sci. Rep.* 3 (2013) 1026.
- Z.Z. You, J.Y. Dong, Surface properties of treated ITO anodes for organic light-emitting devices, *Appl. Surf. Sci.* 249 (2005) 271–276.
- Y.-J. Lin, J.-h. Hong, Y.-C. Lien, B.-Y. Liu, True dipole at the indium tin oxide/organic semiconductor interface, *Appl. Phys. Lett.* 89 (2006) 262110.
- F. Petraki, S. Kennou, Investigation of the interfaces formed between ITO and metal phthalocyanines (NiPc and CoPc) by photoelectron spectroscopy, *Org. Electron.* 10 (2009) 1382–1387.
- D.J. Coutinho, G.C. Faria, R.M. Faria, H. von Seggern, Dynamics of energy level alignment at ITO/organic semiconductor interfaces, *Org. Electron.* 26 (2015) 408–414.
- P.P. Edwards, A. Porch, M.O. Jones, D.V. Morgan, R.M. Perks, Basic materials physics of transparent conducting oxides, *Dalton Trans.* (2004) 2995–3002.
- A. Wan, J. Hwang, F. Amy, A. Kahn, Impact of electrode contamination on the  $\alpha$ -NPD/Au hole injection barrier, *Org. Electron.* 6 (2005) 47–54.
- S. Sinha, C.-H. Wang, M. Mukherjee, Energy level alignment and molecular conformation at rubrene/Ag interfaces: Impact of contact contaminations on the interfaces, *Appl. Surf. Sci.* 409 (2017) 22–28.
- S. Rentenberger, A. Vollmer, E. Zojer, R. Schennach, N. Koch, UV/ozone treated Au for air-stable, low hole injection barrier electrodes in organic electronics, *J. Appl. Phys.* 100 (2006) 053701.
- J. Hwang, A. Wan, A. Kahn, Energetics of metal–organic interfaces: New experiments and assessment of the field, *Mater. Sci. Eng. R* 64 (2009) 1–31.
- A.-M.B. Al-Ajlony, A. Kanjilal, S.S. Harilal, A. Hassanein, Carbon contamination and oxidation of Au surfaces under extreme ultraviolet radiation: An x-ray photoelectron spectroscopy study, *J. Vacuum Sci. Technol. B* 30 (2012) 041603.
- K. Kuribara, H. Wang, N. Uchiyama, K. Fukuda, T. Yokota, U. Zschieschang, C. Jaye, D. Fischer, H. Klauk, T. Yamamoto, K. Takimiya, M. Ikeda, H. Kuwabara, T. Sekitani, Y.-L. Loo, T. Someya, Organic transistors with high thermal stability for medical applications, *Nature Commun.* 3 (2012) 723.
- T. Yamamoto, K. Takimiya, FET characteristics of dinaphthothienothiophene (DNNT) on Si/SiO<sub>2</sub> substrates with various surface-modifications, *J. Photopolym. Sci. Technol.* 20 (2007) 57–59.
- S. Haas, Y. Takahashi, K. Takimiya, T. Hasegawa, High-performance dinaphthothieno-thiophene single crystal field-effect transistors, *Appl. Phys. Lett.* 95 (2009) 022111.
- T. Yamamoto, K. Takimiya, Facile synthesis of highly  $\pi$ -extended heteroarenes, dinaphtho[2,3-b:2',3'-f]chalcogenopheno[3,2-b]chalcogenophenes, and their application to field-effect transistors, *J. Am. Chem. Soc.* 129 (2007) 2224–2225.
- Y. Hasegawa, Y. Yamada, T. Hosokai, K.R. Koswattage, M. Yano, Y. Wakayama, M. Sasaki, Overlapping of frontier orbitals in well-defined dinaphtho[2,3-b:2',3'-f]thieno[3,2-b]-thiophene and picene monolayers, *J. Phys. Chem. C* 120 (2016) 21536–21542.
- H. Ebata, E. Miyazaki, T. Yamamoto, K. Takimiya, Synthesis, properties, and structures of benzo[1,2-b:4,5-b']bis[b]benzothiophene and benzo[1,2-b:4,5-b']bis[b]benzoselenophene, *Org. Lett.* 9 (2007) 4499–4502.
- K. Takimiya, S. Usui, A. Sato, K. Kanazawa, K. Kawabata, Packing structures of (trialkylsilyl) ethynyl-substituted dinaphtho[2,3-b:2',3'-f]thieno[3,2-b]thiophenes (DNNTs): effects of substituents on crystal structures and transport properties, *J. Mater. Chem. C* 10 (2022) 2775–2782.
- R.S. Sánchez-Carrera, S. Atahan, J. Schrier, A. Aspuru-Guzik, Theoretical characterization of the air-stable, high-mobility dinaphtho[2,3-b:2',3'-f]thieno[3,2-b]-thiophene organic semiconductor, *J. Phys. Chem. C* 114 (2010) 2334–2340.
- S. Mandal, S. Roy, M. Saifuddin, S. Hazra, Hole-injection barrier across the intermolecular interaction mediated interfacial DNNT layer, *Appl. Surf. Sci.* 597 (2022) 153696.
- Q. Wang, S. Jiang, L. Qiu, J. Qian, L.K. Ono, M.R. Leyden, X. Wang, Y. Shi, Y. Zheng, Y. Qi, Y. Li, Interfacial flat-lying molecular monolayers for performance enhancement in organic field-effect transistors, *ACS Appl. Mater. Interfaces* 10 (2018) 22513–22519.
- M. Dreher, D. Bischof, F. Widdascheck, A. Huttner, T. Breuer, G. Witte, Interface structure and evolution of dinaphthothienothiophene (DNNT) films on noble metal substrates, *Adv. Mater. Interfaces* 5 (2018) 1800920.
- S. Mandal, S. Jana, S. Roy, M. Saifuddin, S. Hazra, Molecular dipole layer and alkyl side-chain induced improvement in the energy level alignment and wetting of dinaphthothienothiophene thin films, *J. Chem. Phys. C* 127 (2023) 18176–18184.
- S. Mandal, M. Mukherjee, S. Hazra, Evolution of electronic structures of polar phthalocyanine-substrate interfaces, *ACS Appl. Mater. Interfaces* 12 (2020) 45564–45573.
- M.T. Dang, J. Lefebvre, J.D. Wuest, Recycling indium tin oxide (ITO) electrodes used in thin-film devices with adjacent hole-transport layers of metal oxides, *ACS Sustain. Chem. Eng.* 3 (2015) 3373–3381.
- M. Saifuddin, M. Mukhopadhyay, A. Biswas, L. Gigli, J.R. Plaisier, S. Hazra, Tuning the edge-on oriented ordering of solution-aged poly(3-hexylthiophene) thin films, *J. Mater. Chem. C* 8 (2020) 8804–8813.
- S. Roy, M. Saifuddin, S. Mandal, J.R. Plaisier, S. Hazra, Improved exciton bandwidth and edge-on oriented ordering of donor-acceptor copolymer thin films, *Macromolecules* 56 (2023) 7065–7077.
- I. Horcas, R. Fernández, J.M. Gómez-Rodríguez, J. Colchero, J. Gómez-Herrero, A.M. Baro, WSM: A software for scanning probe microscopy and a tool for nanotechnology, *Rev. Sci. Instrum.* 78 (2007) 013705.
- M. Saifuddin, S. Roy, S. Mandal, S. Hazra, Vibronic states and edge-on oriented  $\pi$ -stacking in poly(3-alkylthiophene) thin films, *ACS Appl. Polym. Mater.* 4 (2022) 1377–1386.
- S. Roy, M. Saifuddin, S. Mandal, S. Hazra, Stearic acid mediated growth of edge-on oriented bilayer poly(3-hexylthiophene) Langmuir films, *J. Colloid Interface Sci.* 606 (2022) 1153–1162.
- L. Chkoda, C. Heske, M. Sokolowski, E. Umbach, F. Steuber, J. Staudigel, M. Stöfel, J. Simmerer, Work function of ITO substrates and band-offsets at the TPD/ITO interface determined by photoelectron spectroscopy, *Synth. Met.* 111 (2000) 315–319.
- H. Yagi, T. Miyazaki, Y. Tokumoto, Y. Aoki, M. Zenki, T. Zaima, S. Okita, T. Yamamoto, E. Miyazaki, K. Takimiya, S. Hino, Ultraviolet photoelectron spectra of 2,7-diphenyl[1]benzothieno[3,2-b][1]benzothiophene and dinaphtho[2,3-b:2',3'-f]thieno[3,2-b]thiophene, *Chem. Phys. Lett.* 563 (2013) 55–57.
- E.L. Strein, D. Allred, Eliminating carbon contamination on oxidized Si surfaces using a VUV excimer lamp, *Thin Solid Films* 517 (2008) 1011–1015.
- H. Mori, K. Takimiya, Efficient photocurrent generation at dinaphtho[2,3-b:2',3'-f]thieno[3,2-b]thiophene/C60 bilayer interface, *Appl. Phys. Express* 4 (2011) 061602.
- T. Breuer, A. Karthäuser, H. Klemm, F. Genuzio, G. Peschel, A. Fuhrich, T. Schmidt, G. Witte, Exceptional dewetting of organic semiconductor films: the case of dinaphthothienothiophene (DNNT) at dielectric interfaces, *ACS Appl. Mater. Interfaces* 9 (2017) 8384–8392.
- R. Takeuchi, S. Izawa, Y. Hasegawa, R. Tsuruta, T. Yamaguchi, M. Meissner, S.-i. Ideta, K. Tanaka, S. Kera, M. Hiramoto, Y. Nakayama, Experimental observation of anisotropic valence band dispersion in dinaphtho[2,3-b:2',3'-f]thieno[3,2-b]thiophene (DNNT) single crystals, *J. Phys. Chem. C* 125 (2021) 2938–2943.
- S.R. Forrest, Ultrathin organic films grown by organic molecular beam deposition and related techniques, *Chem. Rev.* 97 (1997) 1793–1896.
- J.K. Bal, S. Hazra, Time-evolution growth of Ag nanolayers on differently-passivated Si(001) surfaces, *Phys. Rev. B* 79 (2009) 155412.
- A.A. Virkar, S. Mannsfeld, Z. Bao, N. Stingelin, Organic semiconductor growth and morphology considerations for organic thin-film transistors, *Adv. Mater.* 22 (2010) 3857–3875.
- A. Tan, P. Zhang, Tailoring the growth and electronic structures of organic molecular thin films, *J. Phys.: Condens. Matter* 31 (2019) 503001.